Environmental Nanomechanical Testing of Polymers and Nanocomposites

Jian Chen, Ben D. Beake, Hanshan Dong and Gerard A. Bell

Abstract The ever-increasing popularity of nanomechanical testing is being accompanied by the development of more and more novel test techniques and adaptation of existing techniques to work in increasingly environmentally challenging test conditions. Considerable progress has been made and reliable mechanical properties of materials can now be obtained at a range of temperature and surrounding media, greatly aiding development for operation under these environmental conditions. In this chapter several of these developments are reviewed, focussing on their use in the non-ambient nanomechanical testing of polymers and nanocomposites.

1 Introduction

Applications of nanomechanical testing are continually increasing, including for example, characterizing the mechanical properties of advanced materials and systems such as micro/nano-mechanical devices (Beake et al. 2009), hard coatings for engineering tools, thin films in semiconductor (Beake and Lau 2005), advanced polymers (Kranenburg et al. 2009; Chen et al. 2010; Beake et al. 2002a, b) and even biomedical tissues (Chen and Lu 2012; Mencik et al. 2009) etc. The successes can be attributed to three main advantages. Firstly, the technique has a high spatial resolution and depth

J. Chen
Jiangsu Key Laboratory of Advanced Metallic Materials, School of Materials Science and Engineering, Southeast University, Nanjing 211189, China
e-mail: j.chen@seu.edu.cn

B. D. Beake (✉) · G. A. Bell
Micro Materials Ltd, Willow House, Yale Business Village, Ellice Way, Wrexham LL13 7YL, UK
e-mail: ben@micromaterials.co.uk

H. Dong
School of Metallurgy and Materials, University of Birmingham, Birmingham B15 2TT, UK

A. Tiwari (ed.), *Nanomechanical Analysis of High Performance Materials*, Solid Mechanics and Its Applications 203, DOI: 10.1007/978-94-007-6919-9_4,

sensitivity. The obtained information is therefore highly localized within a particular area of interest with less influence from its surroundings, for example, in quantitative assessment of the properties of inclusions in metallic alloys. With the spatial resolution and repositioning accuracy down to submicron scale and better, highly detailed mechanical property mapping can be performed to optimize the materials or system under study, explaining why one early name of such instruments was a mechanical properties microprobe. Moreover, the depth sensitivity is sub-nanometer. Intrinsic mechanical properties of (ever thinner) thin films can be obtained by limiting the penetration depth to avoid/minimise the influence of the substrate or sublayers. Secondly, the load and penetration depth are continuously recorded allowing investigation of basic mechanical properties (hardness and elastic modulus) (Fischer-Cripps 2006), time-dependent behavior (Kranenburg et al. 2009; Oyen 2007; Chen et al. 2010), phase transformations (Chinh et al. 2004), stress–strain behavior, fracture (Beake 2005; Casellas et al. 2007) and fatigue behavior (Beake and Smith 2004). Finally, it is routine to schedule large arrays of test experiments to be run automatically over extended periods. Many properties such as hardness and elastic modulus can be calculated without the necessity for post-test imaging, leading to high efficiency and throughput. The current generation of nanomechanical test instrumentation now can perform additional test techniques, such nanoscratch and nano-impact testing, alongside nanoindentation to provide enhanced capability in a single test instrument or platform. The information with the different tests is quite complementary, e.g. nanoindentation to obtain the hardness and elastic modulus of elastic–plastic materials, nanoscratch tests to evaluate their tribological performance and nano-impact to probe their dynamic high strain rate properties. Even compression or bending experiments can be performed using the positioning accuracy and precise load control of the instrument to investigate elastic deformation, yield and fracture of suspended beams or micropillars.

Theoretical analyses of the relationship between contact load and displacement for flat-punch, spherical, or conical indenters into a linear-elasticsolid were derived by Boussinesq (Johnson 1985), Hertz (Johnson 1985), and Sneddon (1965). Based on Sneddon's work, Oliver and Pharr (Oliver and Pharr 1992) developed a simple method to obtain the elastic modulus and hardness using pyramidal indenters where the unloading behavior is assumed to be entirely elastic. In this popular method it is assumed that no plastic deformation or continuing creep deformation occurs during unloading. The results thus are well-suited for elastic–plastic materials. The slope of the unloading curve at any point is called the contact stiffness. In this analysis, the reduced modulus, E_r, is calculated from the stiffness at the onset of the unloading S and the projected area of contact between the probe and the material A_c as Eq. 1:

$$E_r = \frac{\sqrt{\pi}}{2\beta} \cdot \frac{S}{\sqrt{A_c}} \tag{1}$$

where β is the correction factor for the shape of the indenter (whilst there is some debate, β is commonly taken as 1.034 for the Berkovich indenter geometry).

By careful calibration into a reference material of known elastic properties, the diamond area function can be determined relating the contact depth h_c, to the projected contact area. The initial unloading slope S is obtained by fitting the unloading load–displacement response.

As elastic displacements occur both in the specimen and in the indenter (as the indenter is not completely rigid), the elastic modulus of the sample is calculated from E_r using Eq. 2:

$$\frac{1}{E_r} = \frac{1-\nu^2}{E} + \frac{1-\nu_i^2}{E_i} \tag{2}$$

where E and E_i, ν and ν_i are the elastic modulus and the Poisson ratio of the tested material and indenter, respectively. For diamond indenters, E_i and ν_i are 1141 GPa and 0.07, respectively. The mean pressure or hardness, H, can be calculated as in Eq. 3:

$$H = \frac{P}{A_c} \tag{3}$$

where P is the applied load. The technique has also advanced to have its own ISO standard (14577, Parts 1–4) which identifies four key parameters—force, displacement, instrument compliance, and indenter shape—that influence the quality of the results and provide the necessary methodology to accurately calibrate these. The indentation standard strictly applies to metallic and ceramic materials rather than polymers, although it does include provision for minimizing the influence of creep of metals or alloys on the accuracy of determinations of elastic modulus.

2 Nanomechanical Testing of Polymeric Materials

For polymeric materials, a similar approach to obtain E_r and H can be carried out using the Oliver-Pharr method. However, it assumes the initial unloading is purely elastic which ignores the influence of continuing time-dependent deformation which is always present to some degree in the indentation response of polymeric materials. When the creep is particularly pronounced, a nose-shape can even appear during unloading as demonstrated in Fig. 1 that result in negative S and erroneous E_r (Feng and Ngan 2002).

To counteract this, several methods were proposed in terms of the testing conditions and the analysis. Firstly, the creep behaviour at the onset of the unloading is strongly influenced by the testing conditions, such as hold period (dwell time), peak force and loading rate etc. Selection of appropriate holding period, peak force and loading rate is important (Chudoba and Richter 2001). Additionally that the severity of the effects of the residual creep on the contact stiffness, S, is also a function of the unloading rate (Chudoba and Richter 2001; Feng and Ngan 2002). The higher unloading rate is favorable to minimize creep effects. Thus, there are

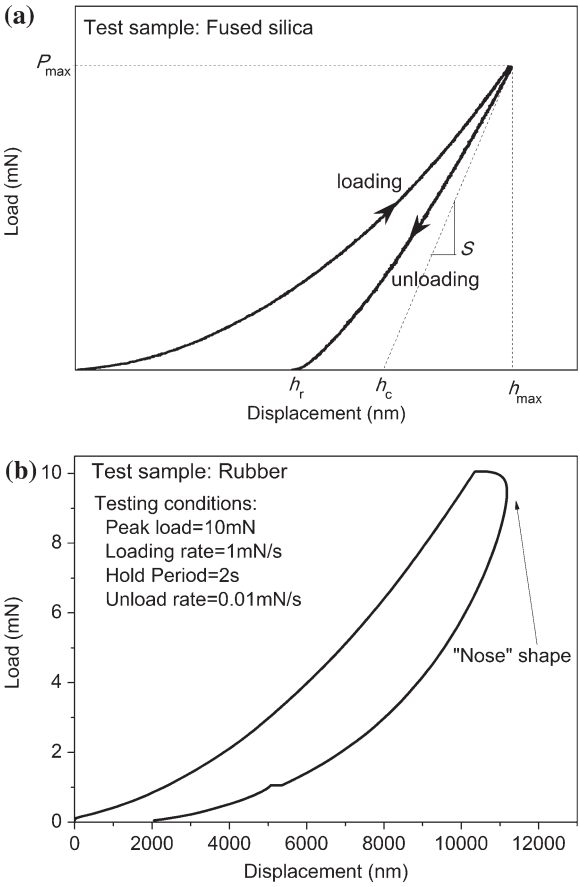

Fig. 1 Indentation load–displacement curves for (**a**) elastic–plastic fused silica, and (**b**) visco-elastic–plastic rubber material

three ways to accommodate the influence of time-dependent deformation on the contact stiffness during the testing (Dasari et al. 2009), (a) increasing the unloading rate, (b) a most common method of holding the indenter at maximum load for a long period of time resulting in a minimum residual creep rate comparing to the unloading rate, and (c) application of an oscillatory force or displacement signal to the tip-sample contact during nanoindentation and measurement of the resultant output signal and phase lag, which are used to obtain the contact stiffness and damping that are analysed to determine the viscoelastic properties of the material (loss and storage moduli, tan delta). This method is sometimes generally called dynamic indentation, or by the instrument manufacturers own terminology such as continuous stiffness measurement (Agilent), nanoDMA (Hysitron) or dynamic mechanical compliance testing (Micro Materials Ltd) etc. Despite its potential, in general good agreement between dynamic indentation and DMA has proved highly challenging for several reasons. Firstly, accurate dynamic calibration of the system is essential as extraction of the material properties requires analysis of the

overall response, which includes the response of the test instrument, especially its damping behavior over the frequency range of interest (Singh et al. 2008). Secondly, reliable extraction of the loss and storage modulus relies on the application of a suitable constitutive equation. For simplicity it is common to assume that the indentation contact can be treated as a linear viscoelastic (Monclus and Jennett 2011), however, it is clear that when pointed (pyramidal, such as Berkovich) indenters are used there is often considerable residual plastic deformation of the polymer surface (Tweedie and Van Vliet 2006). Monclus and Jennett (2011) have critically examined the level of agreement between dynamic indentation and DMA and found poor agreement for a range of polymers, particularly in the loss modulus. They have suggested that more complex models are required to successfully produce loss/viscosity parameters that are equivalent.

A different approach is to account for the creep effects simply by data analysis as proposed in references (Feng and Ngan 2002; Ngan and Tang 2002, 2009). They examined their theoretical model for both linear and power law viscoelastic materials and this model has been shown good reliability for various polymeric materials according to the authors' experience. This correction can be described as in Eq. 4

$$\frac{1}{S} = \frac{1}{S_u} + \frac{\dot{d}_c}{\left|\dot{P}\right|} \tag{4}$$

where S is the contact compliance, S_u is the elastic contact stiffness at the onset of unloading, $\dot{d}_c$ is the displacement derivative at the end of the hold period, and $\left|\dot{P}\right|$ is the unloading rate at the onset of unloading so that the standard contact stiffness equation (Eq. 1) is modified to Eq. 5

$$E_r = \frac{\sqrt{\pi}}{2\beta} \cdot \frac{S_u}{\sqrt{A_c}} \tag{5}$$

The mechanical properties (hardness and elastic modulus) of various polymeric materials like PVC, PMMA, PET, polypropylene (PP), polycarbonate (PC), poly(ethylene oxide) (PEO), poly(acrylic acid) (PAC), nylon 6, nylon 66, rubber, and so forth have been investigated using the nanoindentation technique (Kranenburg et al. 2009; Gray and Beake 2007; Gray et al. 2009; Dasari et al. 2009; Beake et al. 2007). Unsurprisingly the results showed that their mechanical properties are sensitive to the testing conditions including the contact force due to their low stiffness (Kaufman and Klapperich 2009) and peak force, loading rate, unloading rate and hold time due to their rate- and time-dependent properties (Kranenburg et al. 2009). Elastic modulus determinations on polymers are often slightly higher than determined in bulk compression testing, and usually increase as the scale of the contact is reduced (Tweedie et al. 2007).

The creep behavior of the polymers at the nano-/micro-scale is also of intrinsic interest. Several approaches thus have been developed to investigate the creep data collected during nanoindentation with mostly widely used assuming constitutive

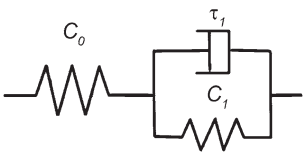

Fig. 2 Schematics of 3-element Kelvin-Voigt model

models (Mencik et al. 2009; Oyen 2005) such as linear viscoelasticity with data fitted to 3-element (Maxwell or Kelvin-Voigt) (Fig. 2) or 4-element (combined Maxwell-Voigt) models.

The instantaneous elasticity, instantaneous plasticity, viscoelasticity and viscoplasticity can be attributed to different physical elements. The creep compliance function is then deduced and the formula between the penetration depth and the applied load can be directly calculated using the Boltzmann integral operator. This methodology has been successfully to simulate the nanoindentation tests. The interested reader can find more details in the references (Mencik et al. 2009; Oyen 2005, 2006, 2007; Oyen and Cook 2009; Chen et al. 2010). Generally speaking, the accuracy of this method strongly depends on the number of the physical elements. In practice a better fit required more variables, which costs more in computation time and relies on a careful selection of the initial value to make the iteration converge.

A semi-empirical logarithmic method has also been used to analyze the dwell data collected at the hold period (Beake 2006; Berthoud et al. 1999; Chen et al. 2010). The logarithmic equation can be expressed as Eq. 6 Beake (2006); Chen et al. (2010)

$$\Delta d = A \ln\left(\frac{t_h}{\tau_L} + 1\right) \tag{6}$$

where Δd and t_h are the increase in depth and hold time during hold period, A and τ_L are termed the extent parameter and the time constant, respectively. The creep strain (ε) can be termed as $\Delta d/d(0)$ where $d(0)$ is the initial depth at the hold period. $A/d(0)$ (Beake 2006) or ($\varepsilon_e/\varepsilon(0)$) (Beake et al. 2007) is termed as the creep strain sensitivity.

The logarithmic equation has been found to closely fit short-time experimental indentation creep data of a wide range of polymeric materials under different testing conditions. The fitting is successful but only two variables—measures of extent A and rate τ_L—are used to describe the visco-deformation behavior. This method can be used not only for linear viscoelastic materials, but also non-linear viscoelastic materials, and with the quality of the fit it is possible to predict the creep response over a relatively long time. However, its limitations are that it is empirical and lacks explicit physical meaning. It is also not possible to deconvolute the particular contributions of elasticity, plasticity, viscoelasticity and viscoplasticity by this approach (Chen et al. 2010).

Similar works have been gradually carried out on the polymer nanocomposites, such as nylon 66/clay (Shen et al. 2004a, b), nylon 12/clay (Phang et al. 2005), epoxy/CNT (Li et al. 2004), nylon 6/CNT (Liu et al. 2004), photopolymer/SiO_2

(Xu et al. 2004), acrylonitrile/butadinene/styrene (ABS) (Beake et al. 2002) and poly(ehylene oxide)(clay/PEO) (Beake et al. 2002) in recent years. The effects of the nano- and micro-scale fillers are a subject of increasing research. In general the resistance to indentation of these nanocomposites gradually increases with increasing filler loading although there are exceptions and the response is typically non-linear (Dasari et al. 2009).

These nanomechanical tests are normally carried out under ambient conditions that may not be particularly close to the actual working conditions in the application. It is well known that the properties of polymeric materials are highly sensitive to the environment. For example, temperature can play an important role. A system may operate efficiently at one temperature and fail when the temperature is changed (Beake 2011; Chen et al. 2010; Everitt et al. 2011; Gray and Beake 2007). To address this problem, several approaches have been used to probe the surface properties of materials under conditions that mimic those which they experience in actual service. In the following sections, we will introduce these advanced nanomechanical test methods and their application on polymeric materials

3 Environmental Nanomechanical Testing of Polymeric Materials

3.1 Environmental Nanoindentation

3.1.1 Influence of Temperature

Obviously the test temperature can strongly influence the properties of polymeric materials. For example, amorphous polymers undergo a transition from a rubbery, viscous amorphous liquid, to a brittle, glassy amorphous solid. According to the viscoelasticity theory, the time-depended properties of polymeric materials depended on the free volume available for molecular (segmental) motions (Beake 2006; Beake et al. 2007). When the temperature increase around the glass transition temperature (T_g) can create sufficient free volume to allow molecules to move relative to one another (Beake et al. 2007). It follows that the creep behavior around T_g will be changed.

Beake et al. (2007); Beake (2006) used nanoindentation to systematically investigate the creep behavior of a range of polymer systems including polystyrene (PS), polypropylene (PP), polycarbonate (PC), polyethersulphone (PES), poly(methylmethacrylate) (PMMA), polytetrafluoroethylene (PTFE), poly(ethylene terephthalate) (PET), ultra-high molecular weight polyethylene (UHMWPE), low-densitypolyethylene (LDPE), acrylonitrilebutadiene-styrene (ABS) copolymer, Santoprene® containing ethylene propylene diene monomer (EPDM), Surlyn® 8140, ethylene/methacrylic acid (E/MAA) copolymer. Their creep factors, such as strain rate sensitivity ($\varepsilon_e/\varepsilon(0)$) and creep rate term ($\varepsilon_r$ = 1/time constant) calculated using the logarithmic Eq. (5) were investigated in terms of their numerical distance, y, from T_g which can be defined as Eq. (7):

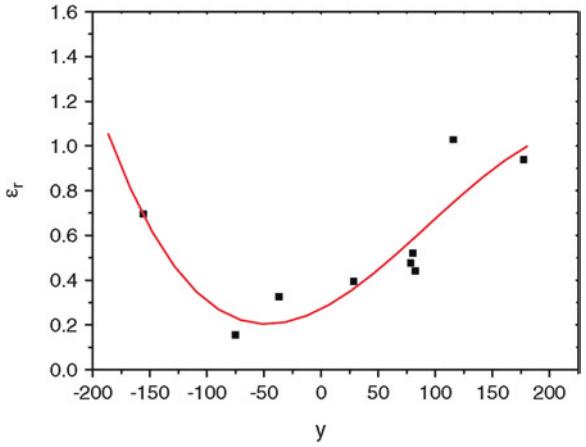

Fig. 3 Creep rate as a function of y defined by Eq. (6) (Beake et al. 2007)

$$y = T_g - T_{exper} \tag{7}$$

Therefore, negative y values correspond to rubber- or liquid-like behavior and positive y values to glassy behavior (Fig. 3).

The change of ε_r with y could be divided into three regions. Firstly, large negative values of y represent the liquid or rubbery region. This implies high v_f values, consequently large chain mobility, and thus high creep rate ε_r. Another is at large positive y values. Polymers are glassy in this region and material brittleness and crack propagation are likely to be the dominant mechanisms of creep, especially for $y > 50$ K or so. In the middle of y range, there is a minimum of ε_r which could be attributed to restricted chain mobility and reduction in brittleness.

To further investigate the effects of temperature on the mechanical properties of polymers, non-ambient temperature tests at both high temperature and low temperature were also carried out. The development of non-ambient temperature nanoindentation can be traced back to 1996 when Suzuki and Ohmura (1996) developed a prototype high-temperature ultra-micro indentation apparatus capable of testing up to 600 °C. However, the test sensitivity of in this prototype was affected by the high testing rates and temperature. Since then, many researchers have made improvements to both the instrumentation and the required experimental methodology (Duan and Hodge 2009). Currently there are three main manufacturers of commercially available systems capable of high temperature nanoindentation testing (1) Hysitron (2) Agilent (previously MTS NanoInstruments) and (3) Micro Materials. The latter's NanoTest has proved popular for this application, with a survey of published papers between 1996 and 2010 reporting around 60 % of published high temperature nanoindentation reports were using it (Everitt et al. 2011). The proportion increased as the test temperature increases above 300 °C (Everitt et al. 2011). There are distinct differences in experimental configuration in the different instruments and these have a direct influence on both the stability and reliability of the test data and the peak temperatures reachable. The Hysitron and Agilent instruments have

a similar vertical loading setup. For example, the Hysitron triboindenter systems used a Peltier thermal element and a resistive heating element as the heating stage. The Peltier thermal element allows for a temperature range from −10 up to 120 °C and with the addition of the resistive element, this testing temperature could be expanded up to 200 °C. By the adoption of a liquid-cooled unit in the resistive heating element, the company has suggested that the temperature can extend to 400 °C (Hysitron 2012). However, a severe limitation of this setup is the use of sample-only heating, particularly for testing at >200 °C. Thermal equilibrium in the contact zone is achieved by holding for a long duration in contact prior to loading. The disadvantage is that as the indentation progresses, it is necessarily involves contact between the colder indenter and the hotter sample.

In the Micro Materials NanoTest nanoindentation system the sample is mounted vertically so that indentation occurs horizontally. The system can be operated to a maximum allowable temperature of up to 750 °C (MicroMaterials 2012). The displacement transducer is placed behind a water/air cooled heat shield to minimize/eliminate radiative heating, and an advantage of the horizontal loading configuration is that convection currents do not transfer significant heat to the displacement measurement electronics. Displacement calibration does not vary within the 25–750 °C temperature range. A key element in its design to reach a much higher working temperature is use of a dual heating strategy (isothermal contact method) where the sample side is heated with a resistance heater and the diamond indenter side is heated up with a small heater with a miniature thermocouple (Everitt et al. 2011; Beake and Smith 2002). This design enables independent heating and control of the sample and the indentation temperatures to minimize the heat flow between the sample and indenter (Fig. 4). Everitt et al. (2011) used finite element modeling to analyse the thermal picture under a diamond indenter with specimen with different conductivities. For the high-conductive materials, a very steep thermal gradient was formed at high temperature which must accommodate their deformation. Through experiments on fused silica up to 600 °C and annealed gold up to 300 °C, they found that the isothermal contact method maintained acceptable thermal drift and produced values of modulus of hardness that compared well with those in literature (Everitt et al. 2011).

It is clear that reliable high-temperature nanoindentation tests require a stable temperature field with minimal thermal flow between the indentation tip and sample, components and surroundings. Design strategies such as heat shielding of components and displacement measuring electronics, isothermal contact by dual heating, long hold period at peak load and relatively large heating blocks for effective heat dissipation from the rest of the sample stage assembly have been employed effectively. Moreover, typically at temperatures in excess of 500 °C, protective gas (e.g. argon purging) may also be necessary to avoid the deterioration of the diamond tip or the sample.

These non-ambient temperature nanoindentation instruments/techniques have been successfully utilized to characterize the mechanical properties of polymers, metals and hard coatings (Beake and Smith 2002; Everitt et al. 2011; Fox-Rabinovich et al. 2006; Gray and Beake 2007, Gray et al. 2009; Lu et al.

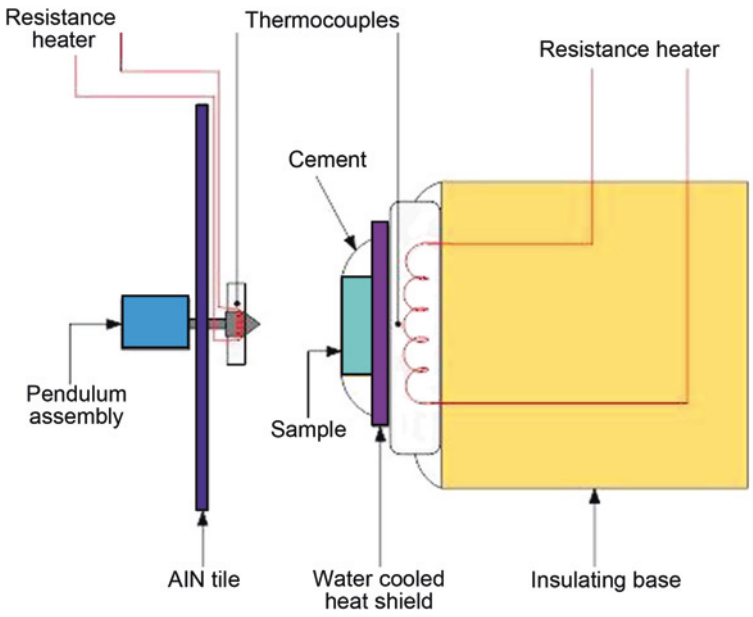

Fig. 4 Schematic of a commercially available high-temperature nanoindenter (NanoTest) employing separate indenter and sample heating and control to achieve isothermal contact

2010; Sawant and Tin 2008; Schuh et al. 2005; Xia et al. 2003; Ye et al. 2005). Encouragingly, it has been found that the properties at measured at non-ambient temperature can reflect their performance at real in-service conditions. For example, the high temperature nanomechanical and micro tribological properties of TiAlN and AlCrN coatings on cemented carbide cutting tool inserts (Fox-Rabinovich et al. 2006) have been correlated directly with their performance in extreme applications such as high speed machining.

Various polymeric materials have been studied using non-ambient temperature nanoindentation. An aerospace polymer resin, PMR-15 polyimide, was investigated by Lu et al. (2010) using a MTS nanoindenter up to 200 °C. Elastic modulus of PMR-15 showed a linear decrease with the increase of the temperature. Gray and Beake (2007), Gray et al. (2009) used the NanoTest to investigate the mechanical properties of PET films with different processing history and crystallinity over the temperature range 60–110 °C. They found that the mechanical properties of undrawn (amorphous) and uniaxially drawn (low crystallinity) PET films dropped quickly at 70–80 °C corresponding to their glass transition temperature, while the properties of biaxially oriented film showed a much more gradual decrease which can be attributed to its high crystallinity. The strain rate sensitivity parameter was also found to be able to characterise the increased time-dependent deformation around the glass transition region. Figure 5a combines measurements taken at room temperature and high temperature on a wide range of amorphous

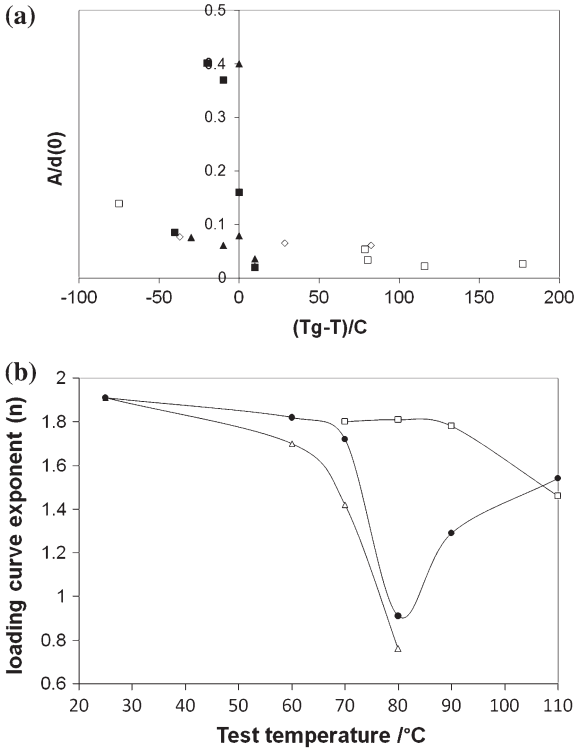

Fig. 5 **a** A/d(0) versus (Tg-T)/ °C from room temperature and high temperature measurements on semicrystalline and amorphous polymeric materials. **b** Variation in loading exponent n for PET films around their glass transition temperature range

and semi-crystalline polymers. It shows a dramatic peak at a temperature a few degrees above T_g, consistent with a maximum in the tan delta peak (which is usually offset by a similar amount from T_g determined from the inflexion of the storage modulus vs. T curve in DMA). Associated with this dramatic increase in A/d(0) is a marked decrease in the exponent n of the loading curve ($P = kd^n$) as shown in Fig. 5b.

Juliano et al. (2007) evaluated the creep compliance of three aliphatic epoxy networks with different molecular weight between crosslink over the temperature range 25–55 °C. They used a 500 μm end radius ruby indenter to generate small contact strains and maintain linear viscoelastic deformation. Tehrani et al. (2011, 2012) studied the nanoindentation creep of nanocomposites of aerospace epoxy and multi-walled carbon nanotubes over the temperature range 25–55 °C using a cBN Berkovich indenter. They determined that the strain rate sensitivity $A/d(0)$ in the nanocomposites decreased relative to the neat epoxy, particularly at elevated temperatures. Interestingly, Li and Ngan have recently reported discrete relaxation events occurring during 600 s hold at 0.9 mN when indented with a Berkovich indenter of end radius 450 nm. Their frequency of occurrence was both crystallinity and temperature dependent. At 30 °C the discrete events (depth steps in creep curves) occurred in under 10 % of tests on LDPE but in over 55 % of tests on

HDPE. At 50 °C the percentage on HDPE was 47 % and at 70 °C the proportion reduced to 40 %. Since the probability increases with crystallinity, the authors suggested the fast relaxation events were likely to arise within the crystalline phase. The reduction in frequency with temperature was considered to be due to enhancement of the viscous flow of the amorphous phase.

Besides the high-temperature application, various engineering activities are carried out at sub-ambient temperatures. These cover winter sports, cryo-machining, marine and aerospace applications (Fink et al. 2008; Iwabuchi et al. 1996; Yoshino et al. 2001; Zhu et al. 1991). For example, the temperature of aircraft tyres can be lower than −50 °C during the aviation cycle. When landing, extremely heavy loads can be applied. Some spacecraft instruments have to be cooled to obtain an improved performance. The materials utilized in the assembly of these electronic circuits can be subjected to mechanical loading.

Adopting the dual-side thermal control approach in the high-temperature test setup, Chen et al. (2010) recently reported the development of a new cold stage accessory based on the NanoTest instrument. The novel nanoindentation capability described demonstrated its ability to investigate the local mechanical properties and the creep behavior of atactic polypropylene down to −30 °C. The sub-ambient temperature cooling system incorporates a purging chamber for eliminating condensation during cooling and two Peltier coolers as shown in Fig. 6 to achieve the isothermal contact. Extended initial contact hold period and low vibration cooling loop were adopted to get vibration free measurements.

Sub-ambient temperature nanoindentation tests have been successfully carried out on atactic polypropylene (aPP) to demonstrate the nanomechanical behaviour through the glass transition temperature, ~18 °C (Chen et al. 2010). It has been found that the hardness and elastic modulus of aPP increased as the test temperature decreased and the amorphous regions went through the glass transition as shown in Fig. 7. The derived creep extent (*A*) using the logarithmic method

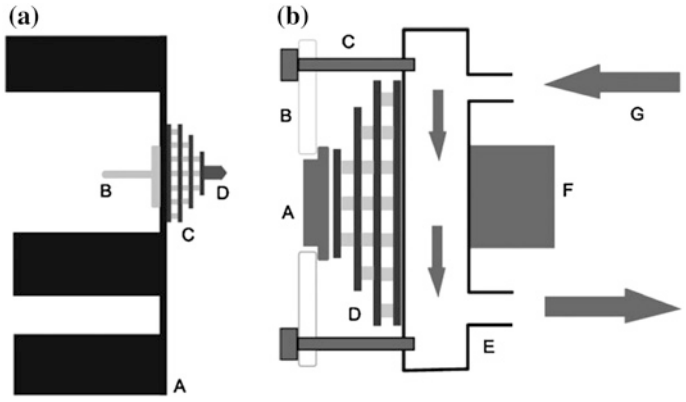

Fig. 6 Schematic diagrams for the cooling systems including (**a**) indenter cooling stack, and (**b**) sample cooling stack (Bell et al. 2011)

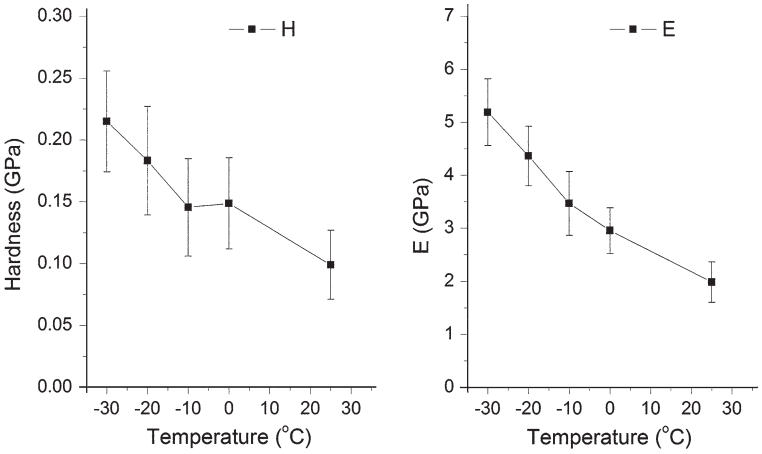

Fig. 7 Hardness and elastic modulus of aPP tested at different temperatures (Chen et al. 2010)

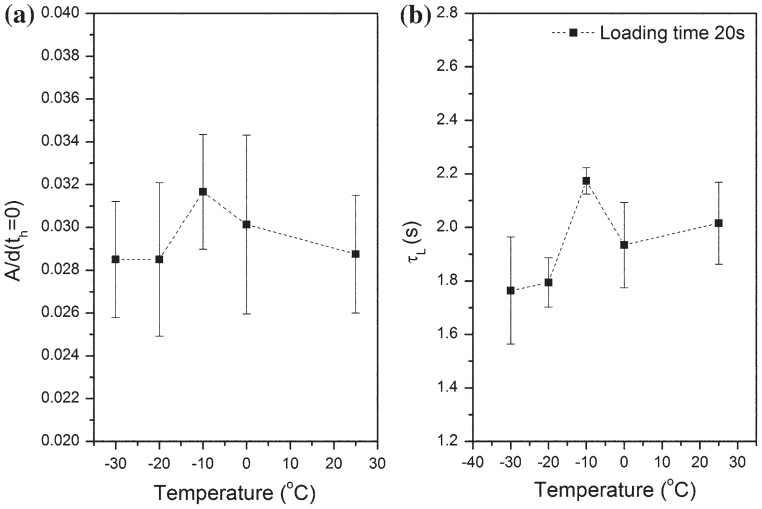

Fig. 8 **a** Creep strain rate sensitivity (A/d(0)) versus test temperature, and **b** creep time constant (τ_L) versus test temperatures fitted using logarithm equation (Chen et al. 2010)

decreased as the temperature was reduced, and for the time constants (τ_L) and strain rate sensitivity ($A/d(0)$) (Fig. 8), there were upper-limit values at −10 °C, about 8 °C above the quoted glass transition temperature.

As yet there are no reports of nanoindentation at temperatures below −50 °C. Cryogenic (down to −150 °C) temperature nanoindentation, however, could be realized using state-of-the-art Joule–Thomson cooling devices (Bell et al. 2011).

As discussed above, it can be seen that the unique ability of nanoindentation to obtain highly spatially resolved quantitative mechanical property measurements could enable microstructural changes in polymeric blends or biomaterials to be studied as a function of temperature. Maxwell and co-workers have recently used high temperature indentation to study the variation in creep compliance across the surface of a polyoxymethylene compression-moulded plate. 16 × 16 grids of indentations with 500 s hold for creep were performed at 23 and 50 °C. Spatially resolved normalized creep compliance maps confirmed that the edges of the moulding showed higher creep compliance. Modulus mapping with the same data showed the edges were also lower in modulus. The polymer at the edges had less time to crystallise due to more rapid cooling at the surface than the bulk, leading to lower crystallinity at the edges, as confirmed by DSC. Their work showed Arrhenius-type behavior, following the relationship between activation energy, temperature and relaxation time (τ) so that when $\ln\tau$ (determined from creep compliance data) is plotted versus 1/T a linear relationship is obtained. Using this approach they showed that by the appropriate Arrhenius shift the 50 °C data overlaid and extended the 23 °C data providing a route for accelerated creep testing.

3.1.2 Influence of Surrounding Media

Besides temperature, the mechanical properties of polymeric samples may vary considerably in different environmental media, such as in air with different humidity or when completely immersed in various fluids. For example, polar materials such as biopolymers [for example DNA, elastin, starch, and cutin (Round et al. 2000)] absorb water and can swell significantly at saturation. Bower (2002) explained that the molecule chain can swell or expand when there is strong attractive interaction between the solvent molecules and the polymer chain. It would be expected that their mechanical properties are interlinked with their water content. Thus it is important to test their mechanical properties and behavior in fluid media rather than to infer from measurements under normal laboratory testing conditions.

One commercial liquid cell system was designed by fitting the nanoindentation platform (Micro Materials Ltd.) with a fluid cell. The fluid cell testing photo is shown in Fig. 9. The potential benefits of the horizontal loading to the fluid testing were summarized (Bell et al. 2008) as (1) the use of an indenter adapter allowing the indenter to be fully immersed in cell, (2) all electronics are well away from the cell, so it can be heated—e.g. to body temperature and above- without risk of steaming of the capacitive displacement sensor, (3) the possibility of fluid exchange during experiment, (4) no significant buoyancy problems, (5) no large change in meniscus position during indentation. Water insoluble samples whose mechanical properties therefore do not vary on immersion in water (fused silica and polypropylene) were used to check the reliability of the setup.

Commercial Nylon-6 samples were tested by Bell and co-workers in deionized water and ambient (50 % relative humidity) conditions (Bell et al. 2008). Typical load–displacement curves are shown in Fig. 10. The hardness and elastic modulus

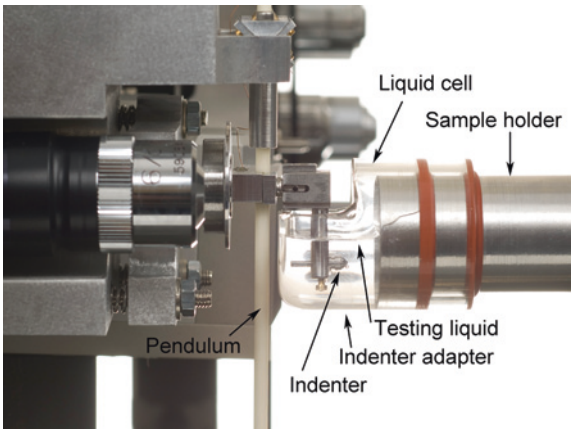

Fig. 9 Schematic of NanoTest fluid cell

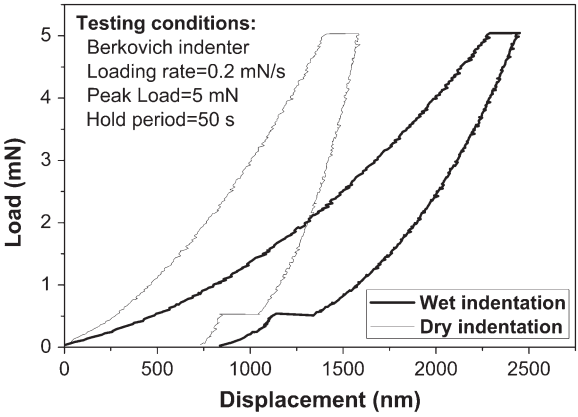

Fig. 10 Typical dry and wet indentation curves for acommercial nylon-6 polymer

measured in deionized water were significantly lower than those measured in ambient conditions. The creep rate sensitivity, $A/d(0)$, decreases significantly in water which is consistent with a decrease in the tan delta peak due to a shift in the glass transition temperature when wet.

Constantinides et al. (2008a, b) tested more compliant hydrogels, finding that the stiffness of PAAm-based electrophoresis gels decreased by a factor of about 1000 when hydrated [E(gel, water) = 270 kPa; E(gel, air) = 300 MPa]. They extended the capability of the fluid cell setup by replacing the diamond Berkovich indenter with a ruby spherical probe of 1 mm diameter chosen to approximate to linear viscoelastic deformation. Using this large radius spherical probe they conducted contact creep experiments on PAAm hydrogels and hydrated porcine skin and liver tissues. 300 s contact creep experiments on porcine skin after 1 h immersion in physiological saline were well fitted by the Kelvin-Voigt model.

Schmidt and co-workers used a NanoTest modified to act as a electrochemical call to study an electroactive polymer nanocomposite thin film containing cationic linear poly(ethyleneimine) and 68 vol % Prussian blue nanoparticles as a candidate stimulus-responsive polymer material (Schmidt et al. 2009). Electrochemical reduction of the Prussian blue particles doubled their negative charge causing an influx of water into the film to maintain electroneutrality. This resulted in swelling and a decrease in elastic modulus. The in situ nanoindentation measurements using a spherical ruby indenter of 5 μm radius showed a reversible decrease in the elastic modulus of the film from 3.4 to 1.75 GPa

Nanoindentation tests have also been performed under vacuum or in different humidities. Korte et al. (2012) have recently described the adaptation of the NanoTest to work in vacuum at temperatures up to 665 °C. Altaf and co-workers recently used the NanoTest with a humidity control unit to study the effect of moisture on the indentation response of a commercial stereolithography polymer resin, Accura 60, over the humidity range 33.5–84.5 % RH (Altaf et al. 2012). Stereo-lithography resins are highly hygroscopic and their mechanical properties are significantly affected by the level of moisture in the environment, with hardness and modulus decreasing with increased moisture in the resin. Transport of moisture from the surface to the bulk took place over a number of days so that a coupled stress-diffusion FEA was required. Gravimetric tests were performed to calculate the diffusion constants and bulk tensile, compressive and creep tensile tests to generate the mechanical material properties for the model. With appropriate modelling, the variation in hardness with (1) increasing penetration into the polymer (2) different environmental conditions could be accurately simulated.

3.2 Environmental Nanoscratch Testing

Since its inception, nanomechanical test instrumentation has developed along modular lines (Beake 2011) with nanoindentation and nanoscratch the two main modules for commercial instruments due to the simplicity to realize both these tests without particularly challenging hardware development. Polymers and polymer-based nanocomposites exhibit various deformation modes in the scratch test such as elastic contact, ironing, ductile ploughing, ductile/brittle machining, tearing, cracking, cutting, fragmentation, etc. (Dasari et al. 2009). In Briscoe and Sinha's review (2003), the most common types of material damage during scratching were illustrated. A combination of different mechanisms is usually operative in any particular contact process. Briscoe and Sinha (2003) developed scratch deformation maps for various polymers at the macro-scale that show clearly how the interplay between cone angle (which alters the contact strain) and normal load produces the different (dominant) scratch mechanisms. More recent work by Brostow and co-workers has shown that, with the exception of highly brittle polymers such as polystyrene, in general the cross-sectional area of the ridges above the scratch can be considerably lower than the cross-sectional area of the scratch groove, presumably due to appreciable densification

alongside ploughing and cutting (Brostow et al. 2007). At the macro-scale there have been efforts to investigate any correlation between scratch hardness and abrasive wear with Sinha and co-workers noting that although PMMA was ~5–6 times harder than UHMWPE its wear resistance were 85 times lower under the same experimental conditions (Sinha and Lim 2006). Nevertheless, despite this, several studies have shown that mechanical properties are strongly implicated in the scratch behaviour of polymers at nano- and micro-scale. Taking advantage of the depth-sensing capability of the nano-/micromechanical test instruments viscoelastic scratch recovery has been shown to be important. A convenient measure of this is the % recovery as defined by Eq. 8:

$$\% \text{ recovery} = 100\,(h_t - h_r)\,/h_t \tag{8}$$

where h_t is the on-load scratch depth and h_r the residual depth. Brostow and co-workers reported a wide variation in recovery after multiple pass micro-scratch experiments with a 200 μm probe (Bermudez et al. 2005a, b). For example, after 15 scans at 15 N viscoelastic recovery on nylon 6 was over 80 % but under 30 % on polystyrene. Similarly wide differences were observed by Sinha and Lim in ~200 μm deep scratches, with PMMA showing 62 % recovery and PP only 36 % (Sinha and Lim 2006). Brostow and co-workers noted that in their multiple micro-scratch tests the residual depths were greater at 1 mm/min than at 15 mm/min for all the thermoplastics they tested (Bermudez et al. 2005). They explained this as the influence of contact heating and greater chain relaxation and viscoelastic recovery at the higher speed. Recovery appears to be linked to tan delta (Brostow et al. 2006) although the relationship was highly non-linear. Beake and Leggett (2002) found that differences in H/E correlated with differences in residual depth and % recovery when scratching PET films of differing crystallinity and orientation at the nano-/micro-scale, at 1mN with a 25 μm end radius probe. When scanning at the nano-scale with a commercial AFM, Beake et al. noticed that aligned ridges formed immediately on uniaxially drawn PET of low hardness and crystallinity at contact forces over 15 nN (Beake et al. 2004) but several scans were required to create similar patterns on harder biaxially drawn PET (Beake and Leggett 2002). These authors suggested that the stick–slip process that leads to the formation of the aligned ridges on the polymer surface proceeded smoothly on the uniaxial PET as the yield threshold for localised plastic deformation is exceeded, whilst the higher crystallinity, H and H/E on biaxial PET has higher yield stress and a more gradual fatigue process over several scans is necessary before the yield stress of the damaged surface was low enough for efficient pattern formation.

In their excellent review, Dasari et al. (2009) noted that factors such as Young's modulus, yield and tensile strength and scratch hardness can all affect the scratch behaviour of polymers and nanocomposites. Surface tension has also been shown to play a role (Brostow et al. 2003). Brostow et al. demonstrated that on increasing the surface tension, friction, penetration and residual depths were also increased. The effects of the additive on the scratch resistance of nanocomposites have also been widely studied. For example, Zeng et al. used nanoindentation, nanoscratch, and nano-tensile tests to study the influence of different contents of fluoropropyl

polyhedral oligomericsilsesquioxane (FP-POSS) in poly(vinylidene fluoride) (PVDF) on the mechanical properties of different systems. Compared with neat PVDF, the scratch resistance of the PVDF/FP-POSS nanocomposites was decreased due to a rougher surface derived from the bigger spherulites. A detailed review can be found in (Dasari et al. 2009).

As demonstrated above, the mechanical properties of the polymers and nanocomposites depend on the specific testing environmental such as temperature, surrounding media. The mechanisms in nano-scratching polymeric materials under non-ambient conditions may vary significantly from those at ambient condition due to the change of their mechanical properties, the surface interaction etc. However, to the knowledge of the authors, the application of non-ambient nanoscratch to polymeric materials is in its infancy although studies of the nanomechanical and tribological properties of diamond-like carbon film at sub-ambient temperatures have revealed significant changes with temperature on this metastable material (Bell et al. 2011; Chen et al. 2011). At the macro-scale Burris, Perry and Sawyer used linear reciprocating pin-on-disk testing to provide evidence for thermal activation of friction (Burris et al. 2007). The friction coefficient of PTFE sliding against 304 stainless steel in nitrogen was measured over the temperature range −80 to +140 °C. They found that in the absence of ice the friction coefficient increased monotonically with decreasing temperature from 0.075 to 0.21, consistent with thermal activation of 5 kJ/mol.

3.3 Environmental Nano-Impact Testing

Constantinides et al. (2008a, b) have noted that whilst the mechanical response of polymeric surfaces to concentrated impact loads is relevant to a range of applications it cannot be inferred from either quasi-static or oscillatory contact loading (i.e. nanoindentation). By modifying the nano-impact module in the NanoTest they were able to assess the strain rate sensitivity of a range of amorphous and semi-crystalline polymers in the velocity range 0.7–1.5 mm/s. Polypropylene and low MW PMMA showed strain rate sensitive impact resistance whilst other polymers (PS, PC, PE, high MW PMMA) did not. They used the coefficient of restitution (e) as a convenient way to assess the energy loss during impact. In an interesting extension of the test capability they performed the nano-impact test on PS and PC over the temperature range 20–180 °C (i.e. from well below to well above their glass transition temperature ranges). They found that e decreased very slightly over the temperature range 0.2–1.0 T/T_g for both PS and PC. However, the capacity of the materials to dissipate the energy of impact greatly (e decreases) increases for temperatures exceeding the glass transition temperature (i.e. $T/T_g > 1$).

Kalcioglu and co-workers have used nano-impact (high strain rate indentation) to assess the response of fully hydrated tissues (from liver and heart) and candidate tissue surrogate materials (a commercially available tissue surrogate and styrenic block copolymer gels) (Kalcioglu et al. 2011). They were able to quantify

resistance to penetration and energy dissipation constants under energy densities of interest for tissue surrogate applications. The nano-impacts were performed at impact rates of 2–20 mm/s. Although the velocity was slow, the energy strain densities were high (0.4–20 kJ/m^3) and comparable with macroscale impact tests such as pneumatic gun and falling weight impacts designed to replicate ballistic conditions (15–60 kJ/m^3) (Kalcioglu et al. 2011). They were able to determine that the energy dissipation capacities of fully hydrated soft tissues were well matched by a 50/50 triblock/diblock composition that was stable in ambient environments.

4 Concluding Remarks

Environmental, or non-ambient, nanomechanical testing has been successfully applied to the characterization of polymers and nanocomposite materials, especially by high temperature nanoindentation. Future directions in nanomechanical test technique development are likely to involve the test envelope being pushed ever outward to map onto more extreme conditions, such as cryogenic temperature, vacuum and various fluid media.

More recently developed nano-scale test techniques, such as nano-scratch or nano-impact, are less well explored than the older nanoindentation test technique. However, performing these tests under non-ambient environmental conditions is a highly promising direction for future research as it enables the tribological and dynamic properties of materials to be studied in nano/micro-scale.

References

Altaf K, Ashcroft IA, Hague R (2012) Modelling the effect of moisture on the depth sensing indentation response of a stereolithography polymer. Comput Mater Sci 52:112–117

Beake BD (2005) Evaluation of the fracture resistance of DLC coatings on tool steel under dynamic loading. Surf Coat Technol 198:90–93

Beake B (2006) Modelling indentation creep of polymers: a phenomenological approach. J Phys D Appl Phys 39:4478–4485

Beake BD (2010) Nanomechanical testing under nonambient conditions. American Scientific Publishers, Los Angeles

Beake BD, Lau SP (2005) Nanotribological and nanomechanical properties of 5–80 nm tetrahedral amorphous carbon films on silicon. Diamond Relat Mater 14:1535–1542

Beake BD, Leggett GJ (2002) Nanoindentation and nanoscratch testing of uniaxially and biaxially drawn poly(ethylene terephthalate) film. Polymer 43:319–327

Beake BD, Smith JF (2002) High-temperature nanoindentation testing of fused silica and other materials. Philos Mag A 82:2179–2186

Beake BD, Smith JF (2004) Nano-impact testing—an effective tool for assessing the resistance of advanced wear-resistant coatings to fatigue failure and delamination. Surf Coat Technol 188–189:594–598

Beake BD, Leggett GJ, Alexander MR (2002a) Characterisation of the mechanical properties of plasma-polymerised coatings by nanoindentation and nanotribology. J Mater Sci 37:4919–4927

Beake BD, Zheng S, Alexander MR (2002b) Nanoindentation testing of plasma-polymerised hexane films. J Mater Sci 37:3821–3826
Beake BD, Shipway PH, Leggett GJ (2004) Influence of mechanical properties on the nanowear of uniaxially oriented poly(ethylene terephthalate) film. Wear 256:118–125
Beake BD, Bell GA, Brostow W et al (2007) Nanoindentation creep and glass transition temperatures in polymers. Polym Int 56:773–778
Beake BD, Goodes SR, Shi B (2009) Nanomechanical and nanotribological testing of ultra-thin carbon-based and MoST films for increased MEMS durability. J Phys D Appl Phys 42:065301
Beake BD (2011) Nanomechanical testing under non-ambient conditions. In: Nalwa HS (ed) Encyclopedia of Nanoscience and Nanotechnology, 2nd edn. Vol. 18. American Scientific Publishers, Valencia, pp 115–120
Bell GA, Bielinski DM, Beake BD (2008) Influence of water on the nanoindentation creep response of Nylon 6. J Appl Polym Sci 107:577–582
Bell GA, Chen J, Dong HS et al (2011) The design of a novel cryogenic nanomechanical and tribological properties instrumentation. Int Heat Treat Surf Eng 5:21–25
Bermudez DM, Brostow W, Carrion-Vilches FJ et al (2005a) Wear of thermoplastics determined by multiple scratching. E-Polymers 001:1–9
Bermudez MD, Brostow W, Carrion-Vilches FJ et al (2005b) Scratch velocity and wear resistance. E-Polymers 003:1–10
Berthoud P, G'Sell C, Hiver JM (1999) Elastic-plastic indentation creep of glassy poly(methyl methacrylate) and polystyrene: characterization using uniaxial compression and indentation tests. J Phys D Appl Phys 32:2923–2932
Bower DI (2002) An introduction to polymer physics. Cambridge Univeristy Press, Cambridge
Briscoe BJ, Sinha SK (2003) Scratch resistance and localised damage characteristics of polymer surfaces—a review. Materialwiss Werkstofftech 34:989–1002
Brostow W, Cassidy PE, Macossay J et al (2003) Connection of surface tension with multiple tribological properties in epoxy plus fluoropolymer systems. Polym Inter 52:1498–1505
Brostow W, Clwnkaew W, Menard KP (2006) Connection between dynamic mechanical properties and sliding wear resistance of polymers. Mater Res Innovations 10:109
Brostow W, Chonkaew W, Rapoport L et al (2007) Grooves in scratch testing. J Mater Res 22:2483–2487
Burris DL, Perry SS, Sawyer WG (2007) Macroscopic evidence of thermally activated friction with polytetrafluoroethylene. Tribol Lett 27:323–328
Casellas D, Caro J, Molas S et al (2007) Fracture toughness of carbides in tool steels evaluated by nanoindentation. Acta Mater 55:4277–4286
Chen J, Lu G (2012) Finite element modeling of nanoindentation based methods for mechanical-properties of cells. J Biomec 45:2810–2816
Chen J, Bell GA, Dong HS et al (2010) A study of low temperature mechanical properties and creep behaviour of polypropylene using a new sub-ambient temperature nanoindentation test platform. J Phys D Appl Phys 43:425404
Chen J, Bell GA, Beake BD et al (2011) Low temperature nano-tribological study on a functionally graded tribological coating using nanoscratch tests. Tribol Lett 43:351–360
Chinh NQ, Gubicza J, Kovacs Z et al (2004) Depth-sensing indentation tests in studying plastic instabilities. J Mater Res 19:31–45
Chudoba T, Richter E (2001) Investigation of creep behaviour under load during indentation experiments and its influence on hardness and modulus results. Surf Coat Technol 148:191–198
Constantinides G, Kalcioglu ZI, McFarland M et al (2008a) Probing mechanical properties of fully hydrated gels and biological tissues. J Biomec 41:3285–3289
Constantinides G, Tweedie CA, Holbrook DM et al (2008b) Quantifying deformation and energy dissipation of polymeric surfaces under localized impact. Mater Sci Eng, A 489:403–412
Dasari A, Yu ZZ, Mai YW (2009) Fundamental aspects and recent progress on wear/scratch damage in polymer nanocomposites. Mater Sci Eng, R 63:31–80

Duan ZC, Hodge AM (2009) High-temperature nanoindentation: new developments and ongoing challenges. JOM 61:32–36
Everitt NM, Davies MI, Smith JF (2011) High temperature nanoindentation—the importance of isothermal contact. Philos Mag 91:1221–1244
Feng G, Ngan AHW (2002) Effects of creep and thermal drift on modulus measurement using depth-sensing indentation. J Mater Res 17:660
Fink M, Fabing T, Scheerer M et al (2008) Measurement of mechanical properties of electronic materials at temperatures down to 4.2 K. Cryogenics 48:497–510
Fischer-Cripps AC (2006) Critical review of analysis and interpretation of nanoindentation test data. Surf Coat Technol 200:4153–4165
Fox-Rabinovich GS, Beake BD, Endrino JL et al (2006) Effect of mechanical properties measured at room and elevated temperatures on the wear resistance of cutting tools with TiAlN and AlCrN coatings. Surf Coat Technol 200:5738–5742
Gray A, Beake BD (2007) Elevated temperature nanoindentation and viscoelastic behaviour of thin poly(ethylene terephthalate) films. J Nanosci Nanotechnol 7:2530–2533
Gray A, Orecchia D, Beake BD (2009) Nanoindentation of advanced polymers under non-ambient conditions: creep modelling and tan delta. J Nanosci Nanotechnol 9:4514–4519
Hysitron (2012) Temperature control stages. http://hysitron.com/products/options-upgrades/temperature-control-stages. Accessed 22 Dec 2012
Iwabuchi, A. and T. Shimizu, et al. (1996). The development of a Vickers-type hardness tester for cryogenic temperatures down to 4.2 K. Cryogenics 36: 75–81
Johnson KL (1985) Contact mechanics. Cambridge University Press, Cambridge
Juliano TF, VanLandingham MR, Tweedie CA et al (2007) Multiscale creep compliance of epoxy networks at elevated temperatures. Exp Mech 47:99–105
Kalcioglu ZI, Qu M, Strawhecker KE et al (2011) Dynamic impact indentation of hydrated biological tissues and tissue surrogate gels. Philos Mag 91:1339–1355
Kaufman JD, Klapperich CM (2009) Surface detection errors cause overestimation of the modulus in nanoindentation on soft materials. J Mech Behav Biomed Mater 2:312–317
Korte S, Stearn RJ, Wheeler JM et al (2012) High temperature microcompression and nanoindentation in vacuum. J Mater Res 27:167–176
Kranenburg JM, Tweedie CA, van Vliet KJ et al (2009) Challenges and progress in high-throughput screening of polymer mechanical properties by indentation. Adv Mater 21:3551–3561
Li XD, Gao HS, Scrivens WA et al (2004) Nanomechanical characterization of single-walled carbon nanotube reinforced epoxy composites. Nanotechnology 15:1416–1423
Liu TX, Phang IY, Shen L et al (2004) Morphology and mechanical properties of multiwalled carbon nanotubes reinforced nylon-6 composites. Macromolecules 37:7214–7222
Lu YC, Jones DC, Tandon GP et al (2010) High temperature nanoindentation of PMR-15 polyimide. Exp Mech 50:491–499
Mencik J, He LH, Swain MV (2009) Determination of viscoelastic-plastic material parameters of biomaterials by instrumented indentation. J Mech Behav Biomed Mater 2:318
MicroMaterials (2012) High and low temperature control. http://www.micromaterials.co.uk/the-nanotest/high-and-low-temperature-control. Accessed 22 Dec 2012
Monclus MA, Jennett NM (2011) In search of validated measurements of the properties of viscoelastic materials by indentation with sharp indenters. Philos Mag 91:1308–1328
Ngan AHW, Tang B (2002) Viscoelastic effects during unloading in depth-sensing indentation. J Mater Res 17:2604–2610
Ngan AHW, Tang B (2009) Response of power-law-viscoelastic and time-dependent materials to rate jumps. J Mater Res 24:853–862
Oliver WC, Pharr GM (1992) An improved technique for determining hardness and elastic modulus using load and displacement sensing indentation experiments. J Mater Res 7:1564–1583
Oyen ML (2005) Spherical indentation creep following ramp loading. J Mater Res 20:2094–2100
Oyen ML (2006) Analytical techniques for indentation of viscoelastic materials. Philos Mag 86:5625

Oyen ML (2007) Sensitivity of polymer nanoindentation creep measurements to experimental variables. Acta Mater 55:3633
Oyen ML, Cook RF (2009) A practical guide for analysis of nanoindentation data. J Mech Behav Biomed Mater 2:396–407
Phang IY, Liu TX, Mohamed A et al (2005) Morphology, thermal and mechanical properties of nylon 12/organoclay nanocomposites prepared by melt compounding. Polym Inter 54:456–464
Round AN, Yan B, Dang S et al (2000) The influence of water on the nanomechanical behavior of the plant biopolyester cutin as studied by AFM and solid-state NMR. Biophys J 79:2761–2767
Sawant A, Tin S (2008) High temperature nanoindentation of a Re-bearing single crystal Ni-base superalloy. Scripta Mater 58:275–278
Schmidt DJ, Cebeci FC, Kalcioglu ZI et al (2009) Electrochemically controlled swelling and mechanical properties of a polymer nanocomposite. ACS Nano 3:2207–2216
Schuh CA, Mason JK, Lund AC et al (2005) High temperature nanoindentation for the study of flow defects. Fundamentals of Nanoindentation and Nanotribology III, Boston
Shen L, Phang IY, Chen L et al (2004a) Nanoindentation and morphological studies on nylon 66 nanocomposites. I. Effect Clay Loading Polym 45:3341–3349
Shen L, Phang IY, Liu TX et al (2004b) Nanoindentation and morphological studies on nylon 66/organoclay nanocomposites. II. Effect Strain Rate Polym 45:8221–8229
Singh SP, Smith JF, Singh RP (2008) Characterization of the damping behavior of a nanoindentation instrument for carrying out dynamic experiments. Exp Mech 48:571–583
Sinha SK, Lim D (2006) Effects of normal load on single-pass scratching of polymer surfaces. Wear 260:751–765
Sneddon IN (1965) The relation between load and penetration in axisymmetric Boussinesq problem for punch of arbitrary profile. Int J Eng Sci 3:47–57
Suzuki T, Ohmura T (1996) Ultra-microindentation of silicon at elevated temperatures. Philos Mag A 74:1073–1084
Tehrani M, Safdari M, Al-Haik MS (2011) Nanocharacterization of creep behavior of multiwall carbon nanotubes/epoxy nanocomposite. Int J Plast 27:887–901
Tehrani M, Al-Haik M, Garmestani H et al (2012) Effect of moderate magnetic annealing on the microstructure, quasi-static, and viscoelastic mechanical behavior of a structural epoxy. J Eng, Mater Technol 134
Tweedie CA, Van Vliet KJ (2006) Contact creep compliance of viscoelastic materials via nanoindentation. J Mater Res 21:1576–1589
Tweedie CA, Constantinides G, Lehman KE et al (2007) Enhanced stiffness of amorphous polymer surfaces under confinement of localized contact loads. Adv Mater 19:2540–2546
Xia J, Li CX, Dong H (2003) Hot-stage nano-characterisations of an iron aluminide. Mater Sci Eng, A 354:112–120
Xu GC, Li AY, De Zhang L et al (2004) Nanomechanic properties of polymer-based nanocomposites with nanosilica by nanoindentation. J Reinf Plast Compos 23:1365–1372
Ye JP, Kojima N, Shimizu S et al (2005) High-temperature nanoindentation measurement for hardness and modulus evaluation of low-k films. Materials, Technology and Reliability for Advanced Interconnects, San Francisco
Yoshino Y, Iwabuchi A, Onodera R et al (2001) Vickers hardness properties of structural materials for superconducting magnet at cryogenic temperatures. Cryogenics 41:505–511
Zhu Y, Okui N, Tanaka T et al (1991) Low temperature properties of hard elastic polypropylene fibres. Polymer 32:2588–2593